Research Square

Preprints are preliminary reports that have not undergone peer review.
They should not be considered conclusive, used to inform clinical practice,
or referenced by the media as validated information.

Direct Damping-Dependent Vertical Ground Motion Model for Stiff Soils in Active Crustal Regions

Héctor Dávalos

hdavalos@up.edu.mx

Universidad Panamericana

Jorge Ruiz-García

Universidad Michoacana de San Nicolás de Hidalgo

David Aguilar

Universidad Panamericana

Research Article

Keywords: Vertical pseudo-acceleration, vertical ground motion model, damping ratio

Posted Date: August 20th, 2026

DOI: https://doi.org/10.21203/rs.3.rs-10297964/v1

License: This work is licensed under a Creative Commons Attribution 4.0 International License.
Read Full License

Additional Declarations: No competing interests reported.

Direct Damping-Dependent Vertical Ground Motion Model for Stiff Soils in Active Crustal Regions

Héctor Dávalos[1], Jorge Ruiz-García[2], and David Aguilar[1]

[1] Universidad Panamericana, Zapopan, México, Facultad de Ingeniería. (ORCID: 0000-0003-3239-1379)
[2] Universidad Michoacana de San Nicolás de Hidalgo, Morelia, México. (ORCID: 0000-0002-7739-8489)

Corresponding author:
Héctor Dávalos: Universidad Panamericana, Zapopan, México, Facultad de Ingeniería.
Email: hdavalos@up.edu.mx

Abstract Although ground-motion prediction models (GMMs) are commonly developed for 5%-damped vertical acceleration response spectra, the damping ratios of many structural and nonstructural systems differ substantially from this conventional value, motivating the development of damping-dependent predictive models. This paper proposes a GMM for estimating vertical pseudo-acceleration response spectra, Sa_v, over a range of damping ratios for shallow crustal earthquakes recorded on stiff soil sites. Moment magnitude and Joyner–Boore distance were considered as predictor variables. The model was developed from a database of 2,408 vertical ground-motion records used to compute Sa_v ordinates at 17 vibration periods between 0.1 and 2.0 s from the linear response of single-degree-of-freedom systems with damping ratios of 1, 2, 5, 10, 15, and 20%. The predictive capability of the introduced GMM is assessed through analyses of model residuals and logarithmic standard deviations. The proposed GMM is further compared with an indirect approach in which the 5%-damped vertical acceleration response spectrum is first estimated using an established GMM and then adjusted through a vertical damping scaling factor model. Both approaches produce comparable estimates of spectral variability. However, median estimates from the proposed model are smaller than those from the indirect method for moderate magnitudes while the opposite holds true in the case of larger magnitude events.

Keywords: Vertical pseudo-acceleration, vertical ground motion model, damping ratio

1. Introduction

Previous studies have demonstrated that the vertical component of earthquake ground motion may have a considerable impact on the seismic performance of structures such as buildings, bridges, and other civil structures, particularly those located close to the fault rupture (e.g., Papazoglou and Elnashai 1996; Elnashai and Papazoglou 1997; Kunnath et al. 2008; Wibowo and Sritharan 2022). For instance, field evidence reported by Papazoglou and Elnashai (1996) indicates that strong vertical shaking can produce pronounced variations in the axial forces of reinforced concrete (RC) columns. These axial force fluctuations may reduce the available shear capacity by decreasing the concrete contribution to shear resistance. In structures with insufficient

confinement or inadequate transverse reinforcement, this phenomenon can trigger brittle compression or compression–shear failures, characterized by longitudinal reinforcement buckling or unexpected diagonal cracking along the column height. These observations highlight the importance of explicitly considering vertical ground motion when assessing the seismic performance of RC buildings and other civil structures, and the estimation of vertical spectral acceleration demands is of outmost importance.

There are two approaches for predicting vertical spectral acceleration ordinates, Sa_v. The first approach to obtain a prediction of Sa_v consists of using an available predictive model for the vertical-to-horizontal spectral acceleration ratio, V/H ratio, and a readily available prediction model for the horizontal spectral acceleration, Sa_H (e.g., Niazi and Bozorgnia 1992; Bommer et al. 2011; Akkar et al. 2014). The second approach consists of predicting directly Sa_v from a ground motion prediction model, GMM (e.g., Niazi and Bozorgnia 1992; Ambraseys and Simpson 1996; Abrahamson and Silva 1997; Campbell 1997; Campbell 2001; Ambraseys and Douglas 2003; Campbell and Bozorgnia 2003; Chiou and Youngs 2013; Bozorgnia and Campbell 2016b; Stewart et al. 2016; Gülerce et al. 2017; Çagnan et al. 2017; Laouami 2019; Phung et al. 2022; Hu et al. 2025; Dominguez et al. 2025). Both approaches would also require a prediction model of a damping scaling factor, DSF, to scale Sa_v ordinates and obtain those corresponding to damping ratios different than 5% (e.g., Akkar et al. 2014; Rezaeian et al. 2012, 2014). The following section details the methodology to obtain Sa_v using both approaches.

To the best of the authors' knowledge, Niazi and Bozorgnia (1992) introduced the first predictive model for the V/H ratio, which showed that it is highly dependent on frequency, source distance, and site conditions. Since then, several GMMs for the V/H ratio have been introduced in the literature. For instance, Malhotra (2006) developed functional forms for the V/H ratio across the acceleration-, velocity-, and displacement-constant regions of a smoothed response spectrum. Bommer et al. (2011) developed a regional GMM for V/H response spectral ratios, which considers moment magnitude (M_w), source-to-site distance, style of faulting (SoF), and site classification as predictor variables. Gülerce and Abrahamson (2011) introduced a GMM of the V/H ratio, which is dependent on the earthquake magnitude and distance, consistent with previous models, but differs from previous studies in that it accounts for the differences in the nonlinear site-response effects on the horizontal and vertical components. Similarly, Akkar et al. (2014) developed a set of compatible ground-motion prediction equations for horizontal and vertical damping scaling factors, together with V/H spectral ratios. Their V/H model predicts the vertical-to-horizontal spectral ratio as a function of M_w, Joyner–Boore distance (R_{jb}), SoF, and a V_{S30}-based nonlinear site function. This model provides a European and Middle Eastern alternative to the Western US-based NGA-West2 models. Bozorgnia and Campbell (2016a) developed a comprehensive ground-motion model for V/H response spectral ratios utilizing the NGA-West2 database, which considers moment magnitude, fault rupture distance, style of faulting, and shallow site conditions as predictor variables across an extended range of structural periods up to 10 seconds.

Similarly, the earliest GMM for the DSF factor was introduced by Abrahamson and Silva (1996), which highlighted that the vertical DSF factors are linearly magnitude-dependent. Their DSF model is valid for 18 specific spectral periods ranging from 0.02 to 5.0 seconds and provided coefficients for 9 damping ratios between 0.5% and 20%. Years later, McGuire et al. (2001) introduced a novel approach based on random

vibration theory for scaling 5% damped Sa_v spectra to 8 damping levels between 0.5% and 20% (ζ =0.5%, 1%, 2%, 3%, 7%,10%, 15% and 20%), where the DSF is based on strong motion duration, which is a distance- and magnitude-dependent variable. Rezaeian et al. (2012, 2014) established an empirical model for spectral DSFs across both horizontal and vertical components, utilizing M_w, source-to-site distance, and period-dependent variables to adjust baseline 5% damped spectral acceleration ordinates to damping ratios between 0.5% and 30%.

As mentioned previously, several GMMs for predicting directly Sa_v ordinates have been introduced in the literature which as customarily, were developed from the linear response of systems having 5% damping ratio. In the authors' knowledge, the first predictive equation for vertical peak ground acceleration was developed by Niazi and Bozorgnia (1991), who employed a dataset of over 700 accelerograms recorded from 12 earthquakes in northeast Taiwan. The predictive equation is based on earthquake magnitude (either local magnitude or seismic wave magnitude) and hypocentral distance as predictive parameters. In a follow-up study, Niazi and Bozorgnia (1992) extended their study to predict vertical spectral acceleration, whose functional form incorporates a logarithmic distance saturation term, and independent coefficients for different soil types (i.e., Holocene, Pleistocene, rock) and focal mechanisms. Similarly, Ambraseys and Simpson (1996) introduced a GMM for predicting vertical peak ground acceleration and vertical spectral acceleration at 46 periods of vibration between 0.1 and 2.0 s. Their model was based on a European ground motion dataset of 411 earthquake records, whose predictor variables are the seismic wave magnitude (M_s) (between 4.0 and 7.9), source-to-site distance, and the site geology (i.e., rock, stiff soil, and soft soil sites). Abrahamson and Silva (1997) introduced a GMM for vertical spectral acceleration that distinguishes between the hanging wall and footwall effects of dipping faults, as well as nonlinear soil response. In a subsequent study, Ambraseys and Douglas (2003) introduced a GMM for vertical spectral acceleration employing a ground motion dataset of 186 strong-motion records recorded within 15 km of the surface projection of earthquakes with M_s between 5.8 and 7.8. The spectral response of the vertical acceleration and the attenuation of its spectral ordinates with magnitude and distance differ in amplitude and shape from those of the horizontal acceleration. Based on previous works by Campbell (1997) and Campbell and Bozorgnia (2003), Bozorgnia and Campbell (2016b) developed a comprehensive GMM for Sa_v using the NGA-West2 database for shallow crustal events up to a distance of 300 km, whose functional form captures complex scaling features, including explicit magnitude-dependent hypocentral depths, refined hanging-wall models, and nonlinear site response functions. Particularly, Stewart et al. (2016) concluded that the vertical component should preferably be modeled directly, rather than obtained indirectly through a V/H ratio, especially because the vertical component exhibits attenuation, site effects, and aleatory variability that are not identical to those of the horizontal component. It should be noted that previous GMMs for Sa_v focused on the seismic response of 5%-damped linear systems.

The objective of this paper is to introduce a GMM for estimating Sa_v across multiple damping ratios for shallow crustal earthquakes events on stiff soils. For this purpose, a relatively large ground motion set consisting of 2,408 vertical earthquake records was employed to compute Sa_v ordinates at 17 natural periods of vibration, between 0.1s and 2.0s, from the linear response of single-degree-of-freedom systems having 6 different damping ratios, ζ(ζ=1, 2, 5, 10, 15, and 20%). The adequacy of the moment magnitude and Joyner-Boore

distance predictive parameters in the GMM is examined in terms of the logarithmic standard deviation and the residuals of the estimations. A comparison of the prediction of Sa_v using the introduced GMM with respect to Sa_v predicted with an indirect approach consisting of the Bozorgnia and Campbell (2016b) GMM for the 5%-damped Sa_v ordinates and the Rezaeian et al. (2014) vertical damping scaling factor model is also presented in this paper.

2. Indirect versus Direct models to estimate Sa_v.

Previous research has developed ground motion models and predictive equations in active crustal regions that can be implemented towards the final objective of estimating vertical pseudo-acceleration ordinates, Sa_v, with damping ratios smaller and larger than 5% (e.g., Boore and Atkinson 2008, Campbell and Bozorgnia 2008; Chiou and Youngs 2008; Akkar et al. 2014; Campbell and Bozorgnia 2016). Note that these models estimate different definitions of the pseudo-acceleration horizontal component (e.g., random component, GMRotI50 component, RotD50 component, etc). Using these models, either two or even three intermediate steps are required before the median Sa_v for a damping ratio other than 5% can be estimated.

The first option involves a larger process. Initially, horizontal GMMs are used to estimate the 5%-damped pseudo-acceleration spectral ordinate for a given definition of the horizontal component. Then, V/H models (e.g., Campbell and Bozorgnia 2003; Malhotra 2006; Gülerce and Abrahamson 2011; Bommer et al. 2011; Bozorgnia and Campbell 2016a; Ramadan et al. 2021) are used to convert horizontal ordinates to their vertical counterparts. Finally, a vertical damping scaling factor (DSF) model (e.g., Abrahamson and Silva 1996; McGuire et al. 2001; Rezaeian et al. 2014) is implemented to estimate the Sa_v ordinates with the desired damping ratio. Mathematically, the median estimation of Sa_v for a period of vibration, T, and a damping ratio, ζ, following this process is:

$$Sa_V(T,\zeta) = Sa_H(T,\zeta = 5\%,\theta) \cdot \frac{V}{H}(T,\zeta = 5\%) \cdot DSF_v(T,\zeta) \quad (1)$$

where Sa_H $(T,\zeta = 5\%,\Theta)$ corresponds to the horizontal component of 5%-damped pseudo-spectral acceleration, for a period, T, and a set of causal parameters (Θ), as required by the specific GMM used in the Sa_H estimation, $V/H(T,\zeta = 5\%)$ is the vertical-to-horizonal ratio from a 5%-damped predictive model, and $DSF_v(T,\zeta)$ is the applicable vertical damping scaling factor as a function of T and the desired damping ratio.

For many performance-based applications, the variance of Sa_v, σ_{lnSaV}, is also required. In this case, to estimate this parameter, one needs to combine the individual logarithmic standard deviations of Sa_H, Sa_v, and the DSF_v along with the correlations of the residuals between these three random variables. Equation 2 presents the corresponding formula.

$$\sigma^2_{lnSa_V(T,\zeta)} = \sigma^2_{lnSa_H} + \sigma^2_{\ln(\frac{V}{H})} + \sigma^2_{ln\ DSFv} + 2\rho_{1,2} \cdot \sigma_{lnSa_H} \cdot \sigma_{\ln(\frac{V}{H})} + 2\rho_{1,3} \cdot \sigma_{lnSa_H} \cdot \sigma_{ln\ DSFv} + 2\rho_{2,3} \cdot \sigma_{\ln(\frac{V}{H})} \cdot \sigma_{ln\ DSFv} \quad (2)$$

where $\sigma^2_{lnSa_H}$ corresponds to the variance of the logarithmic horizontal component of pseudo-acceleration, $\sigma^2_{\ln(\frac{V}{H})}$ corresponds to the variance of the vertical-to-horizontal ratio, $\sigma^2_{ln\ DSFv}$ corresponds to the variance of the

vertical damping scaling factor, $\rho_{1,2}$ to the correlation coefficient between $ln\, Sa_H$ and $ln(\frac{V}{H})$, $\rho_{1,3}$ to the correlation coefficient between $ln\, Sa_H$ and $\ln DSF_V$, and $\rho_{2,3}$ to the correlation coefficient between $ln(\frac{V}{H})$ and $ln\, DSF_v$. Note that the dependence of the lognormal random variables Sa_H, V/H, and DSF_v on T, damping ratio, and causal parameters in equation 2 has been dropped for simplicity.

It should be noted that Gülerce and Abrahamson (2011) considered the correlation between the residuals of $ln\, Sa_H$ and the $ln\,(V/H)$ models in the propagation of uncertainty when constructing 5%-damped vertical acceleration design spectra. Rezaian et al. (2012) reported correlation coefficients for distances R_{rup} shorter than 50 km, between $ln\, Sa_H$ and the logarithm of the horizontal *DSF* ($ln\, DSF_H$) using active crustal region earthquake events, and more recently using subduction interface and intraslab events (Rezaeian et al. 2021). Rezaiean et al. (2014) mentioned that the correlation between $ln\, Sa_V$ and $ln\, DSF_V$ could be approximated using the one corresponding to $ln\, Sa_H$ and $ln\, DSF_H$, however, the specific correlation between $ln\, Sa_H$ and $ln\, DSF_V$ seems to be unavailable. Additionally, to the best of the authors' knowledge, there are currently no correlation models between $ln\,(V/H)$ and $ln\, DSF_V$.

This process becomes large and cumbersome and requires three correlation models that leads to propagation uncertainty and increase the parametric uncertainty in the process. Moreover, some of this correlation coefficients are not readily available or are limited in their applicability. Clearly one can ignore the correlation terms, but this assumption introduces epistemic uncertainty to the results and can lead to either over- or underestimations of Sa_v spectral ordinates.

The second option is more straightforward as it only involves the use of an Sa_V GMM and a vertical *DSF*. This option eliminates the need of a Sa_H GMM, a V/H ratio model, and the corresponding correlation coefficient. The median and variance of Sa_V following this approach is shown in equations 3 and 4.

$$Sa_V(T,\zeta) = Sa_V(T,\zeta = 5\%,\theta) \cdot DSF(T,\zeta) \tag{3}$$

$$\sigma^2_{lnSa_V(T,\zeta)} = \sigma^2_{lnSa_V(T,5\%,\theta)} \cdot \sigma^2_{ln\ DSFv(T,\zeta)} \cdot 2\rho_{4,3}\sigma_{\ln Sav(T,5\%)}\sigma_{ln\ DSFv(T,\zeta)} \tag{4}$$

where $\rho_{4,3}$ corresponds to the correlation coefficient between $ln\, Sa_V$ and the $ln\, DSF_V$ previously mentioned.

As an alternative to this two first options, this study aims to develop a model that directly estimates Sa_v without the need to use either Sa_H, a V/H model, and/or vertical *DSF* models. Thus, the propagation of uncertainty is avoided. Moreover, one does not need to assume independence between random variables, nor one needs to assume that the correlation coefficients between $ln\, Sa_V$ and $ln\, DSF_V$ could be approximated by the correlation between $ln\, Sa_H$ and $ln\, DSF_H$ as subtly implied by Rezaeian et al. (2014), even when they were computed using only records with R_{rup} < 50 km or for Sa_H spectral ordinates.

3. Ground Motion Records and Spectral Periods

Strong-motion accelerometer data used in this investigation was obtained from the NGA West-2 Database (Ancheta 2014). Thus, all ground motion records are previously processed and baseline corrected. The main database of strong motion records selected in this study comprises 2,408 vertical acceleration records obtained from events with moment magnitudes, M_w, larger than 5.5, and Joyner-Boore distances shorter than 300 km. Additionally, all those ground motions were recorded in stations located on sites with V_{s30} values between 180 and 360 m/s. In other words, all of them are classified as site class D according to NEHRP. This ground motion selection has the objective of focusing on this quite common site class in major cities which is actually the default site class that ASCE 7-16 stipulates when site-specific geotechnical boring data or shear-wave velocities are not available. Moreover, by focusing on this site class we avoid highly non-linear soil amplifications that could occur on soft soils or peculiar behavior of extremely stiff soils or rock sites.

Careful consideration of minimum usable frequencies leads to a different number of ground motions used for periods between 0.01 and 2.0 s. A total of 2,408 vertical ground motion records were analyzed for the shortest vibration period, compared to 2,348 for the longest. Specifically, the periods used herein are 0.01, 0.02, 0.03, 0.05, 0.075, 0.10, 0.15, 0.20, 0.25, 0.30, 0.40, 0.5, 0.75, 1.0, 1.5, and 2.0 s. This range of periods is the same, up to a period of 2.0 s, than the one used by Rezaeian et al. (2014) and is focused on the spectral region where most structures (except for long-period structures such as bridges) can be affected by vertical accelerations. For this study, elastic response spectra for the vertical component of the ground motions have been computed for critical damping ratios, ζ, of 1, 2, 5, 10, 15, and 20%.

Figure 1 presents M_w-R_{jb} scatterplots of the data. Subfigure a) presents the information corresponding to a period of vibration of 0.1 s whereas subfigure b) presents the information corresponding to T_n = 2.0 s.

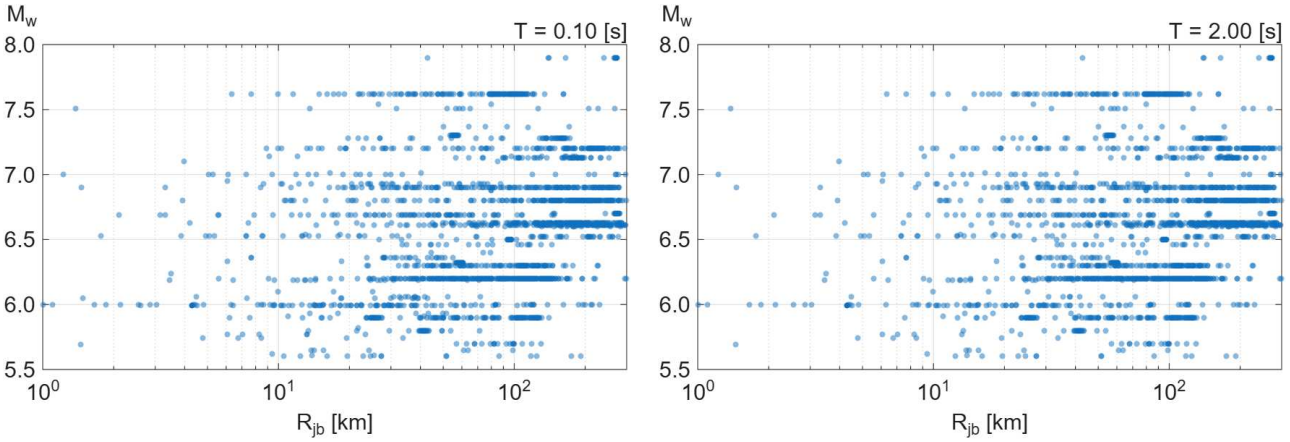


***Figure* 1.** *R_{jb} vs M_w scatter plot of the ground motions used in this study for two periods of vibration. Left: T = 0.1 s; and Right: T = 2.0 s.*

4. Methodology

This study proposes a ground motion model for the logarithmic mean and logarithmic standard deviation of the vertical pseudo-acceleration (Sa_v) of periods between 0.01 and 2.0 s and six critical damping ratios between

1% and 20%. The model is a function of M_w and R_{jb}, as well as a set of six coefficients specifically tailored for each damping ratio. Preliminary analyses were conducted using additional predictor variables such as faulting mechanism, hypocentral depth, or the depth to the 2.5 km/s horizon. Yet, minor improvements in the model were obtained with their inclusion. Specifically, the consideration of faulting mechanism yielded an average reduction in variability of 1.8% across the considered periods of vibration while the other variables had an even smaller influence. Thus, it was decided to maintain a simpler functional form, reducing the parametric uncertainty.

The proposed model estimates the natural logarithm of vertical pseudo-acceleration ordinates, $ln\, Sa_V$, for different damping ratios as:

$$ln\, Sa_V = f(T, M_w, R_{jb}) + \varepsilon + \eta \quad (5)$$

where $f(T,M_w,R_{jb})$ represents the logarithmic mean of Sa_v, ε the within-event term and η the between-event term. Note that in this model, the two latter variables are assumed to be normally distributed random variables with zero mean and standard deviations equal to ϕ and τ, respectively. In Eq. 5, the logarithmic mean is divided into two terms, the event and the path term, referred to as F_E and F_P, respectively. These two terms are presented in the following subsections.

A mixed-effects model (Brillinger and Preisler 1984; Brillinger and Preisler 1985; Abrahamson and Youngs 1992) was used to estimate the coefficients of the functional form, which is a simplified version of the functional form proposed by Bozorgnia and Campbell (2016b).

4.1 The Event and Path Functions

The event scaling function is given by:

$$F_E = b_1 + b_2 \cdot M_w + b_3 \cdot max(M_w - 6.5, 0)^2 \quad (6)$$

where the coefficients b_1, b_2, and b_3 were obtained independently for each period of vibration and damping ratio using the mixed-effects regression procedure.

The second scaling function, the path-dependent one is given by:

$$F_P = b_4\, ln\left(\sqrt{\{R_{\{jb\}}^2 + (b_5 \cdot M_w)^2\}}\right) + b_6 \cdot R_{\{jb\}} \quad (7)$$

where b_4, b_5, and b_6 were also computed for each period and critical damping ratio.

4.2 Variability of the model

The total logarithmic standard deviation of the model, σ, is period-dependent and given by:

$$\sigma = \sqrt{\phi^2 + \tau^2} \quad (8)$$

where ϕ corresponds to the within-event variability and τ to the between-event variability. While the former refers to the contribution to the total variability coming from ground motion records from the same event at different sites, the latter corresponds to the contribution of different events having the same M_w.

5. Performance of the Ground Motion Model

5.1 Median estimations

Figure 2 presents the median Sa_v estimations for T = 0.1 and 2.0 s as a function of R_{jb}, for three different values of M_w and four selected critical damping ratios. These figures demonstrate that the proposed model follows the overall trends and the reduction in Sa_v values with increases in distance and/or damping ratio or with reductions in M_w. Empirical data from representative magnitude ranges is also included in the figure.

Elastic response spectra of Sa_v ordinates are shown in Figure 3 for four different M_w-R_{jb} pairs and for the six damping ratios under study. As expected, regardless of the damping ratio, all response spectra start with the same amplitude, and their increase/decrease depends on the period of vibration and damping ratio. A small jaggedness in the response spectra is seen, and it is more evident at low damping ratios and large magnitudes. These minor variations are a result of the nonlinear regression process but overall represent adequately the variation in Sa_v with period of vibration and/or critical damping ratio.

5.2 Quantification of variability

A comparison of the logarithmic standard deviation as a function of period of vibration and for the six damping ratios is shown in Figure 4. As expected, lower damping ratios tend to exhibit larger variabilities, and these are slightly larger for periods of vibration between 0.03 and 0.2 s and for the largest period under study than for the rest of the periods of vibration. Larger damping ratios (i.e., 10-20%) tend to have more stable variabilities. These range from 0.57 to 0.72 with average logarithmic standard deviations of 0.65, 0.64, and 0.63 for damping ratios of 10%, 15%, and 20%, respectively. A comparison of the variabilities between the proposed model and the indirect method using the Bozorgnia and Abrahamson (2016b) Sa_v GMM and the Rezaeian et al. DMF (2014) will be presented in the next section.

5.3 Residuals

The residuals are an important result as they help to evaluate the adequacy of the model. Within-event residuals, ε, plotted as a function of R_{jb}, for damping ratios of 2% and 10%, and for periods of vibration of 0.1, 0.5, 1.0 and 2.0 s are presented in Figure 5. Binned means and the 95% confidence intervals (CI) were computed every 20 km, and a linear regression of the data is also shown in a dashed green line. The lack of a significant trend in the residuals suggests the adequacy of the functional form.

Figure 6 presents the between-event residuals, η, as a function of M_w for the same damping ratios and periods shown in the previous figure. Again, the figure presents binned means and the 95% CI's every 0.5 magnitude units, and a linear regression of the data shown in a dashed green line. Note that the linear regression of the data suggests no clear trend, indicating the functional form used for magnitude scaling does not introduce significant bias. Similar results were obtained for other periods of vibration and damping ratios.

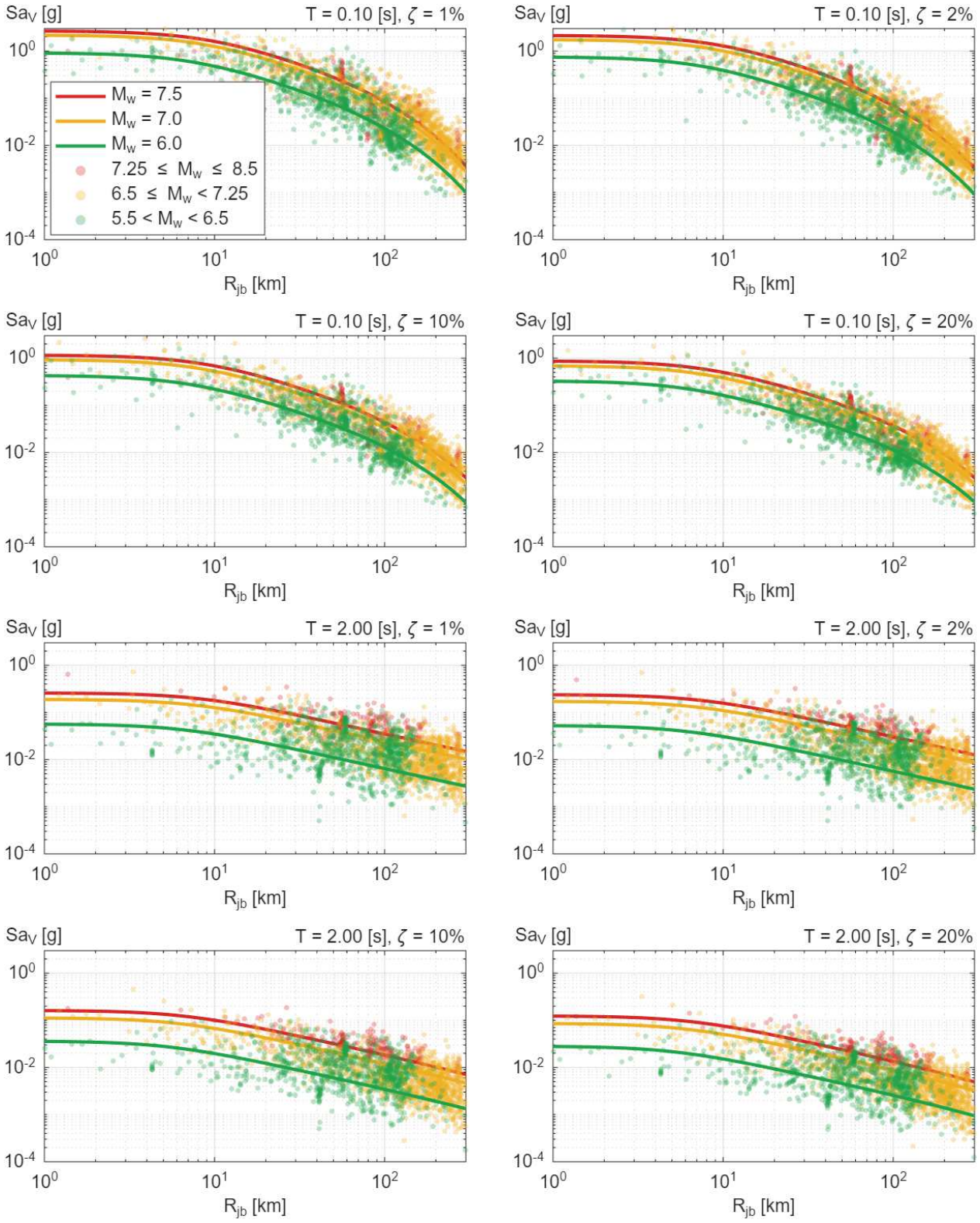
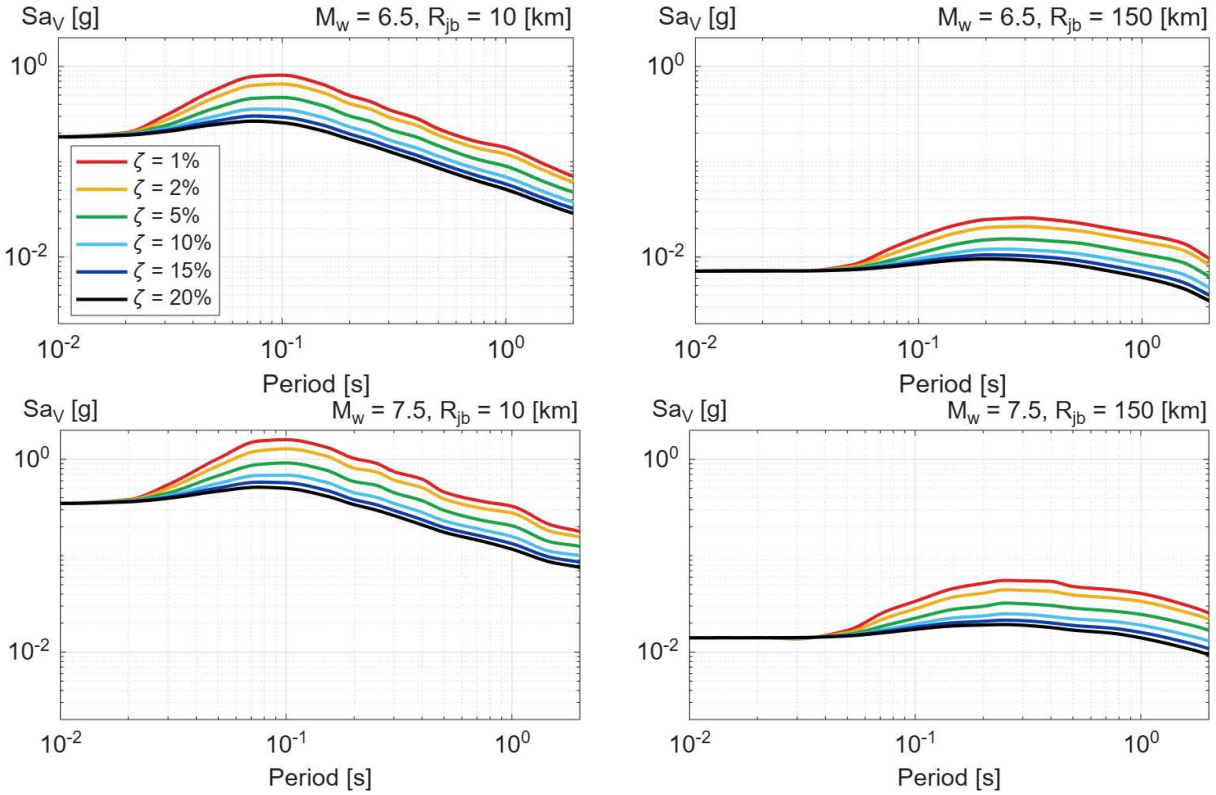


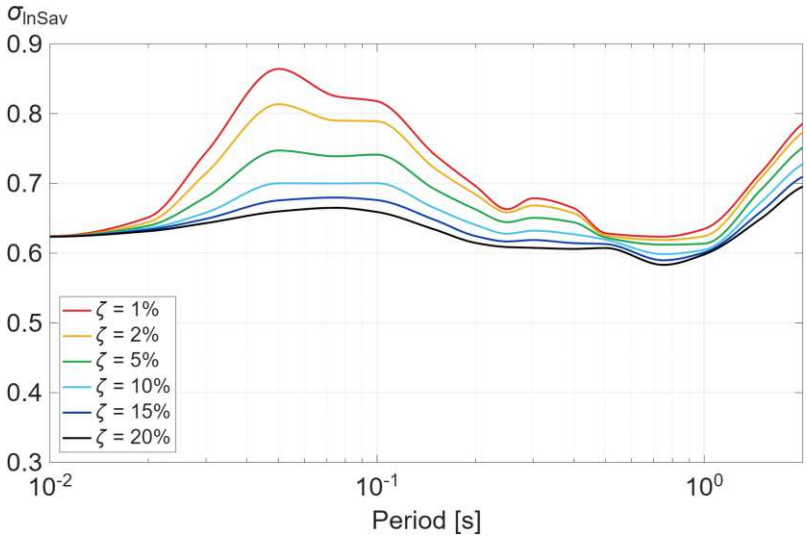
Figure 2. *Median predictions of the GMM as a function of M_w and R_{jb} for T = 0.1 and 2.0 s and damping ratios equal to 1, 2, 10, and 20%.*



274

275

276 ***Figure 3.*** *Median Sa_V spectra for the six damping ratios and four different M_w-R_{jb} pairs.*

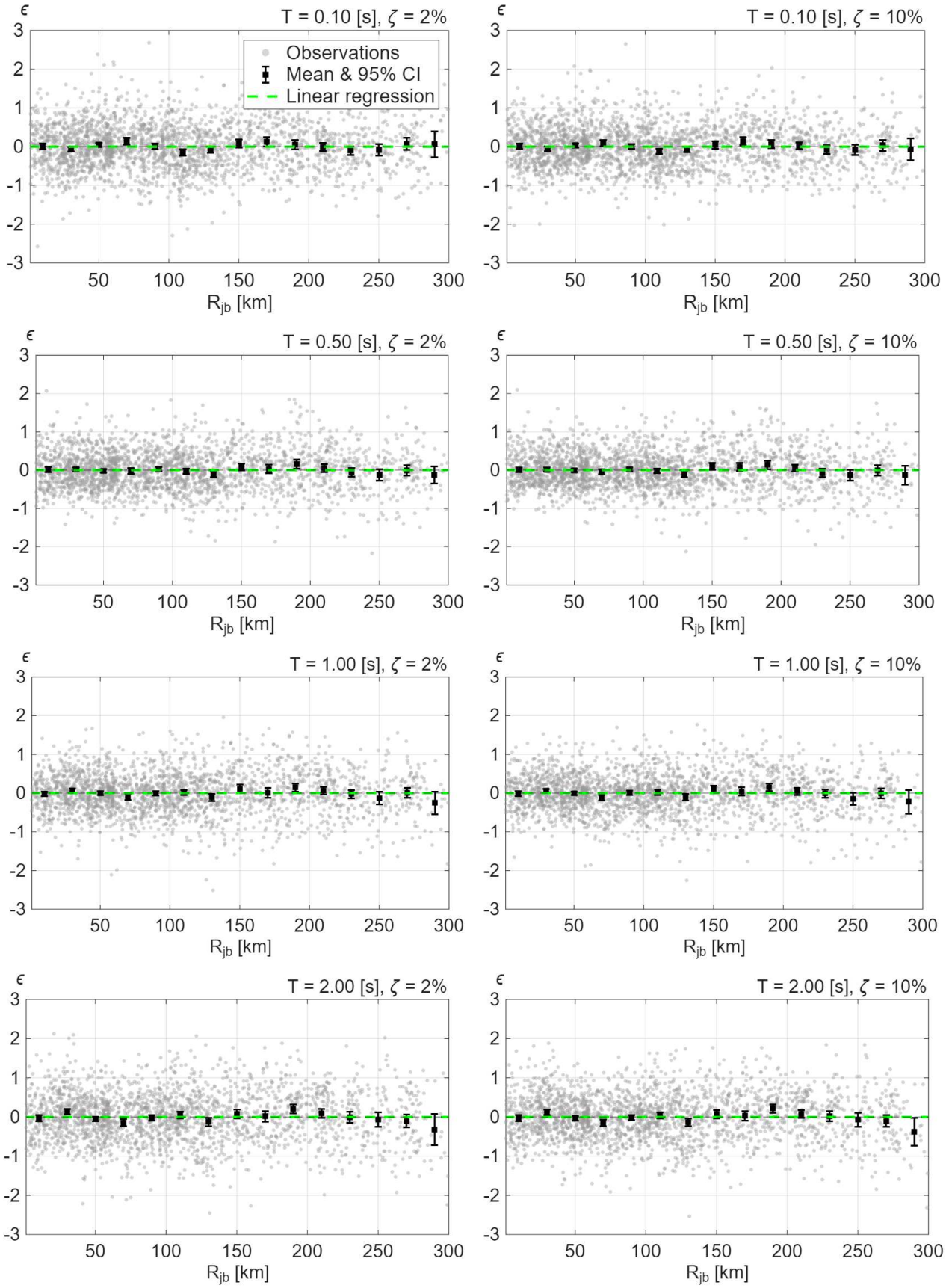


277

278 ***Figure 4.*** *Logarithmic standard deviation of the proposed model as a function of period and damping ratio.*

279 5.4 Coefficients of the model

280 Tables 1 through 6 present the resulting coefficients, for damping ratios of 1, 2, 5, 10, 15, and 20%,
281 respectively. These coefficients are suitable for the prediction of Sa_v median ordinates as a function of M_w, R_{jb},
282 ζ, and the period of vibration. The units used for the distance terms are km and the Sa_v ordinates are estimated
283 as a function of gravity. Moreover, these tables also present the period-dependent values for ϕ, τ, and σ.



284

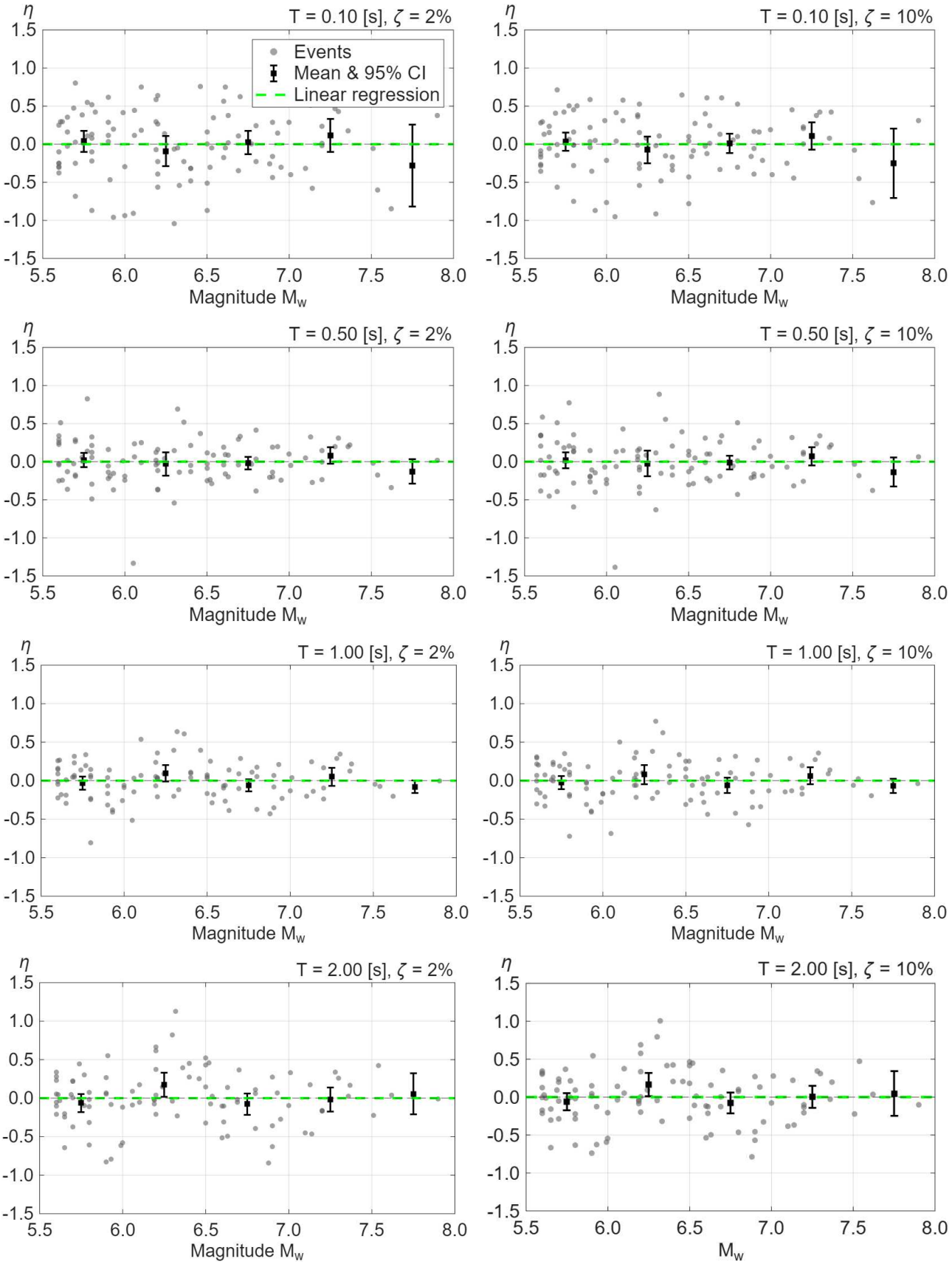
285

286

287

288 ***Figure 5.*** *Within-event residuals of the ln(Sa_v) as a function of R_{jb} for 2 and 10% critical damping ratio and*

289 *four periods of vibration. Binned means using a distance range of 20 km are shown in black.*



290

291

292

293

294 ***Figure* 6.** *Between-event residuals of the ln(Sa_v) as a function of M_w for 2 and 10% critical damping ratio and*

295 *four periods of vibration. Binned means using a distance range of 0.5 Mw are shown in black.*

Table 1. Coefficients of the median vertical ground motion model for 1% damping

T (sec)	b_1	b_2	b_3	b_4	b_5	b_6	τ	ϕ	σ
0.010	-5.48224	0.92851	-0.24680	-0.89246	0.86850	-0.00683	0.48	0.40	0.62
0.020	-5.22930	0.91485	-0.24365	-0.92501	0.84506	-0.00674	0.49	0.43	0.65
0.030	-4.56659	1.00722	-0.34728	-1.20730	1.30859	-0.00581	0.54	0.52	0.74
0.050	-4.01021	1.13346	-0.41943	-1.39861	1.86025	-0.00763	0.62	0.60	0.86
0.075	-4.87510	1.23521	-0.45967	-1.22595	1.67056	-0.00936	0.62	0.54	0.82
0.10	-4.84159	1.11960	-0.38237	-1.00641	1.16319	-0.01013	0.62	0.54	0.82
0.15	-4.98161	1.00116	-0.25684	-0.76039	0.83187	-0.01024	0.59	0.44	0.74
0.20	-5.56127	0.98757	-0.25064	-0.61404	0.62629	-0.00987	0.57	0.40	0.70
0.25	-5.80163	1.00043	-0.21842	-0.61323	0.70338	-0.00868	0.55	0.36	0.66
0.30	-5.96792	0.96244	-0.20443	-0.53181	0.44709	-0.00854	0.56	0.39	0.68
0.40	-6.03776	0.94113	-0.14970	-0.53570	0.52941	-0.00735	0.53	0.40	0.66
0.50	-5.97871	0.86694	-0.13452	-0.47005	0.33859	-0.00714	0.53	0.34	0.63
0.75	-6.42346	0.89762	-0.08087	-0.50503	0.38972	-0.00543	0.53	0.32	0.62
1.0	-7.47992	1.05360	-0.20616	-0.54610	0.48578	-0.00456	0.55	0.32	0.63
1.5	-7.90856	1.08022	-0.26665	-0.61136	0.67712	-0.00205	0.60	0.39	0.72
2.0	-10.06271	1.44581	-0.47505	-0.79578	1.07289	0.00008	0.65	0.44	0.79

Table 2. Coefficients of the median vertical ground motion model for 2% damping

T (sec)	b_1	b_2	b_3	b_4	b_5	b_6	τ	ϕ	σ
0.010	-5.47452	0.92718	-0.24480	-0.89249	0.86918	-0.00683	0.48	0.40	0.62
0.020	-5.27128	0.91745	-0.24297	-0.92084	0.84950	-0.00674	0.48	0.43	0.64
0.030	-4.83478	0.98480	-0.31826	-1.11199	1.14591	-0.00622	0.52	0.49	0.71
0.050	-4.37324	1.10602	-0.40147	-1.30324	1.63710	-0.00752	0.59	0.56	0.81
0.075	-4.73057	1.17825	-0.42416	-1.23008	1.63189	-0.00864	0.60	0.52	0.79
0.10	-4.84760	1.09334	-0.35976	-1.02305	1.16785	-0.00958	0.60	0.52	0.79
0.15	-4.99838	0.98045	-0.25015	-0.78132	0.82349	-0.00983	0.58	0.43	0.72
0.20	-5.60439	0.96854	-0.26832	-0.62712	0.61465	-0.00964	0.56	0.39	0.68
0.25	-5.79796	0.97744	-0.22023	-0.62921	0.71348	-0.00850	0.55	0.37	0.66
0.30	-5.90062	0.93009	-0.19164	-0.54952	0.45271	-0.00839	0.54	0.39	0.67
0.40	-5.99597	0.91392	-0.15790	-0.55015	0.51298	-0.00733	0.52	0.40	0.66
0.50	-6.09434	0.86591	-0.14568	-0.48337	0.34093	-0.00715	0.52	0.35	0.63
0.75	-6.53582	0.89387	-0.09328	-0.51316	0.36249	-0.00544	0.52	0.33	0.62
1.0	-7.52682	1.03900	-0.19669	-0.55274	0.47229	-0.00462	0.54	0.32	0.62
1.5	-8.18159	1.09215	-0.28296	-0.59883	0.57999	-0.00229	0.59	0.39	0.71
2.0	-10.06234	1.41493	-0.44040	-0.78038	0.96268	-0.00010	0.63	0.44	0.77

296

Table 3. Coefficients of the median vertical ground motion model for 5% damping

T (sec)	b_1	b_2	b_3	b_4	b_5	b_6	τ	ϕ	σ
0.010	-5.46948	0.92616	-0.24343	-0.89240	0.86930	-0.00683	0.48	0.40	0.62
0.020	-5.33321	0.92377	-0.24700	-0.91729	0.86005	-0.00674	0.48	0.42	0.64
0.030	-5.05970	0.95974	-0.28564	-1.02364	1.01234	-0.00658	0.50	0.46	0.68
0.050	-4.79223	1.05965	-0.36329	-1.17063	1.35127	-0.00739	0.55	0.50	0.75
0.075	-4.79928	1.09946	-0.37122	-1.16251	1.42508	-0.00803	0.56	0.48	0.74
0.10	-4.82929	1.03861	-0.31747	-1.02226	1.15924	-0.00876	0.56	0.48	0.74
0.15	-5.09767	0.95248	-0.24264	-0.79800	0.83281	-0.00922	0.55	0.42	0.69
0.20	-5.65118	0.93807	-0.25784	-0.65162	0.63137	-0.00915	0.54	0.39	0.66
0.25	-5.92730	0.95384	-0.22117	-0.63982	0.65330	-0.00822	0.53	0.37	0.64
0.30	-6.02388	0.91201	-0.18237	-0.57158	0.45811	-0.00812	0.52	0.39	0.65
0.40	-6.09719	0.89014	-0.16005	-0.56504	0.47960	-0.00719	0.50	0.40	0.64
0.50	-6.19471	0.85180	-0.14686	-0.51210	0.34854	-0.00690	0.50	0.37	0.62
0.75	-6.78335	0.89399	-0.10763	-0.52436	0.34650	-0.00541	0.50	0.35	0.61
1.0	-7.65608	1.01231	-0.18228	-0.55069	0.42348	-0.00466	0.52	0.32	0.61
1.5	-8.54269	1.10678	-0.28271	-0.60366	0.51234	-0.00235	0.58	0.38	0.69
2.0	-10.03581	1.37470	-0.38376	-0.78763	0.91390	-0.00018	0.61	0.44	0.75

Table 4. Coefficients of the median vertical ground motion model for 10% damping

T (sec)	b_1	b_2	b_3	b_4	b_5	b_6	τ	ϕ	σ
0.010	-5.46626	0.92518	-0.24233	-0.89211	0.86881	-0.00682	0.48	0.40	0.62
0.020	-5.38599	0.92912	-0.25056	-0.91397	0.86351	-0.00675	0.48	0.42	0.64
0.030	-5.22907	0.95541	-0.27458	-0.98044	0.96243	-0.00672	0.49	0.43	0.66
0.050	-5.01602	1.01375	-0.32191	-1.07120	1.15601	-0.00732	0.52	0.46	0.70
0.075	-4.89529	1.03406	-0.31995	-1.08812	1.25403	-0.00761	0.53	0.46	0.70
0.10	-4.95837	0.99622	-0.28236	-0.98744	1.09413	-0.00812	0.54	0.45	0.70
0.15	-5.19268	0.92151	-0.21643	-0.79752	0.81987	-0.00861	0.53	0.41	0.66
0.20	-5.75462	0.92081	-0.24131	-0.67313	0.65631	-0.00852	0.51	0.38	0.64
0.25	-6.06517	0.93341	-0.21116	-0.64481	0.62828	-0.00789	0.51	0.37	0.63
0.30	-6.06203	0.88566	-0.15377	-0.59329	0.47732	-0.00769	0.50	0.38	0.63
0.40	-6.24025	0.87189	-0.15794	-0.56846	0.44727	-0.00698	0.49	0.39	0.63
0.50	-6.31599	0.83770	-0.13076	-0.52898	0.35702	-0.00664	0.49	0.38	0.62
0.75	-7.10402	0.91007	-0.11289	-0.53338	0.35078	-0.00539	0.49	0.35	0.60
1.0	-7.86095	1.00517	-0.16961	-0.55755	0.39117	-0.00452	0.51	0.33	0.60
1.5	-8.78902	1.11234	-0.26803	-0.61915	0.50550	-0.00232	0.56	0.38	0.67
2.0	-10.06059	1.33778	-0.33574	-0.77983	0.86375	-0.00046	0.59	0.42	0.73

297

Table 5. Coefficients of the median vertical ground motion model for 15% damping

T (sec)	b_1	b_2	b_3	b_4	b_5	b_6	τ	ϕ	σ
0.010	-5.46349	0.92418	-0.24128	-0.89169	0.86809	-0.00681	0.48	0.40	0.62
0.020	-5.40854	0.92985	-0.25006	-0.91026	0.86305	-0.00677	0.48	0.41	0.63
0.030	-5.28099	0.94829	-0.26569	-0.95917	0.94302	-0.00678	0.49	0.43	0.65
0.050	-5.12631	0.98912	-0.29782	-1.02198	1.06528	-0.00723	0.51	0.44	0.68
0.075	-4.99223	0.99722	-0.28694	-1.03487	1.15354	-0.00743	0.52	0.44	0.68
0.10	-5.05045	0.96454	-0.25357	-0.95130	1.02656	-0.00781	0.52	0.43	0.68
0.15	-5.29844	0.90607	-0.20578	-0.79220	0.80243	-0.00815	0.51	0.40	0.65
0.20	-5.82764	0.90843	-0.22346	-0.68148	0.66437	-0.00811	0.50	0.37	0.62
0.25	-6.15066	0.91955	-0.20327	-0.64684	0.60421	-0.00762	0.49	0.37	0.62
0.30	-6.15849	0.88081	-0.15907	-0.60641	0.49373	-0.00736	0.49	0.38	0.62
0.40	-6.38085	0.86769	-0.15526	-0.57174	0.44532	-0.00676	0.48	0.39	0.61
0.50	-6.47405	0.84030	-0.12763	-0.53995	0.37234	-0.00642	0.48	0.38	0.61
0.75	-7.27779	0.91545	-0.11456	-0.54301	0.35816	-0.00526	0.48	0.34	0.59
1.0	-7.96305	0.99836	-0.16596	-0.56771	0.38805	-0.00433	0.50	0.34	0.60
1.5	-8.95590	1.12006	-0.25928	-0.63571	0.52627	-0.00227	0.55	0.37	0.66
2.0	-10.11214	1.32201	-0.32086	-0.78125	0.85197	-0.00061	0.58	0.41	0.71

298

Table 6. Coefficients of the median vertical ground motion model for 20% damping

T (sec)	b_1	b_2	b_3	b_4	b_5	b_6	τ	ϕ	σ
0.010	-5.46063	0.92312	-0.24005	-0.89115	0.86721	-0.00681	0.48	0.40	0.62
0.020	-5.41323	0.92813	-0.24729	-0.90711	0.86263	-0.00678	0.48	0.41	0.63
0.030	-5.34128	0.94695	-0.26318	-0.94413	0.92764	-0.00682	0.49	0.42	0.64
0.050	-5.22304	0.97631	-0.28544	-0.98937	1.01246	-0.00716	0.50	0.43	0.66
0.075	-5.06454	0.97054	-0.26323	-0.99495	1.08729	-0.00732	0.50	0.43	0.66
0.10	-5.14918	0.94620	-0.23827	-0.92406	0.97734	-0.00759	0.51	0.42	0.66
0.15	-5.42308	0.90077	-0.20108	-0.78575	0.79343	-0.00781	0.50	0.39	0.63
0.20	-5.89959	0.90224	-0.20992	-0.68800	0.66977	-0.00778	0.49	0.37	0.61
0.25	-6.17076	0.90401	-0.18992	-0.65083	0.59448	-0.00736	0.48	0.37	0.61
0.30	-6.25276	0.88068	-0.15994	-0.61739	0.51584	-0.00707	0.48	0.38	0.61
0.40	-6.49335	0.86812	-0.15034	-0.57963	0.44700	-0.00654	0.47	0.38	0.61
0.50	-6.60108	0.84606	-0.12535	-0.55363	0.39613	-0.00617	0.47	0.38	0.61
0.75	-7.42026	0.92108	-0.11179	-0.55185	0.36150	-0.00511	0.48	0.34	0.58
1.0	-8.06627	0.99793	-0.16723	-0.57846	0.38993	-0.00412	0.49	0.34	0.60
1.5	-9.09117	1.12678	-0.25836	-0.64717	0.53560	-0.00225	0.54	0.36	0.65
2.0	-10.17600	1.31416	-0.31764	-0.78293	0.84994	-0.00070	0.57	0.40	0.70

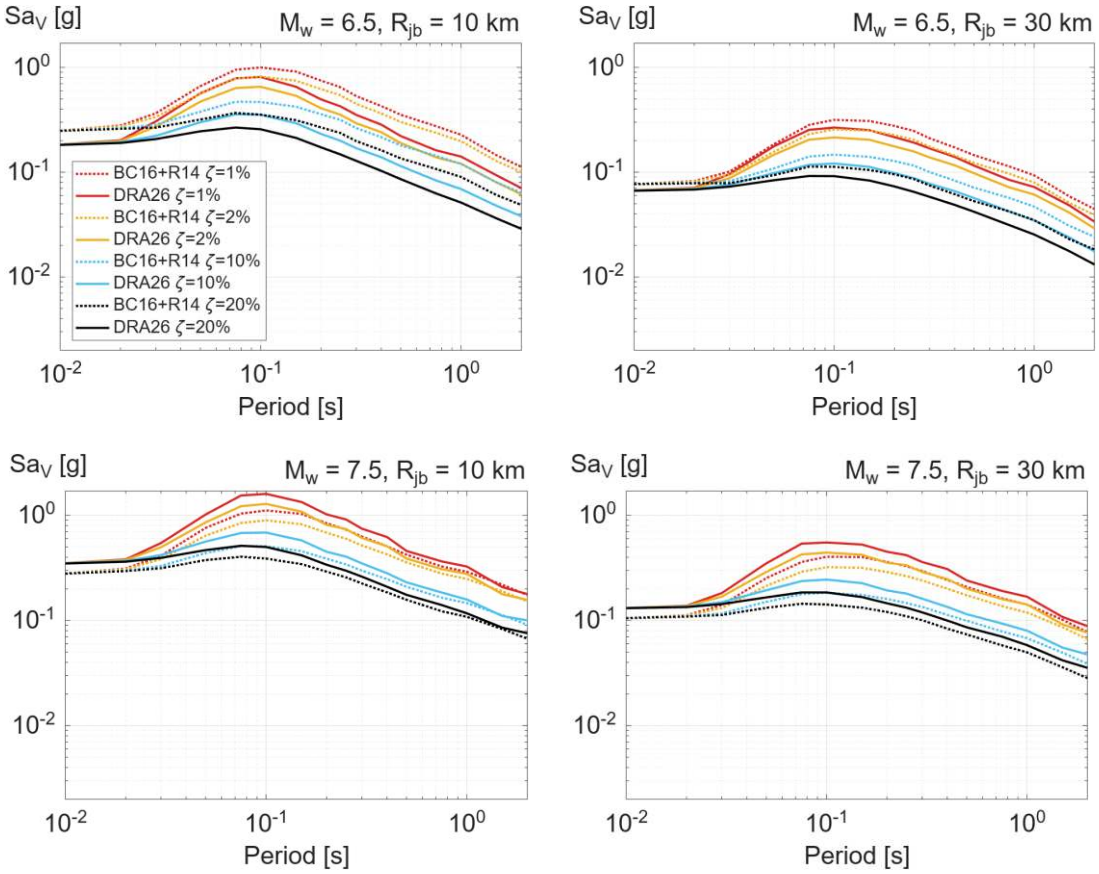
5.5 Median and variability comparison with indirect method

One of the benefits of the proposed damping-dependent GMM is the ability to compute Sa_v ordinates directly by using a single functional form. This is instead of a two- or even a three-step process that relies on GMMs for the Sa_H, the V/H ratio, and a *DSF* model along with their corresponding correlations.

In this section, we present a comparison between the proposed model, termed as DRA26 hereafter, and a two-step process involving the Bozorgnia and Campbell (2016b) GMM for the 5%-damped Sa_v ordinate and the Rezaeian et al. (2014) vertical DSF model, termed BC16+R14. For comparison purposes, the BC16+R14 model considers a V_{s30} value of 270 m/s (mid-range value of the NEHRP site class D), a Z_{hyp} of 10 km consistent with the average Z_{hyp} of the ground motion database used in the study, a strike-slip faulting mechanism, ignoring the c_{12} and c_{13} terms strictly applicable to the Japanese geology, with $k_2 = 0$, and also ignoring deep basin effects.

Figure 7 presents the median estimations of the proposed model, DRA26, and those corresponding to the BC16+R14 compound model for four R_{jb}-M_w scenarios and 1, 2, 10, and 20% damping ratios. For comparison purposes we consider scenarios with M_w = 6.5 and 7.5, and R_{jb} distances of 10 and 30 km. Overall trends from the two models are similar, but smaller amplitudes of Sa_v ordinates are obtained with the proposed GMM in the case of the moderate magnitude scenario, and this difference seems to reduce as distance increases. These smaller amplitudes can reach values 43% smaller than those computed with the BC16+R14 compound model but have averages across the whole spectral region, damping ratios, and the two scenarios considered of 31.4 and 18.6% for the shortest and longest distances, respectively. In the case of the large magnitude scenario, the proposed model yields larger Sa_v ordinates. These can be up to 48% larger than their BC16+R14 counterparts but are on average between 19.9% and 23.9% larger for the shortest and longest distances, respectively.

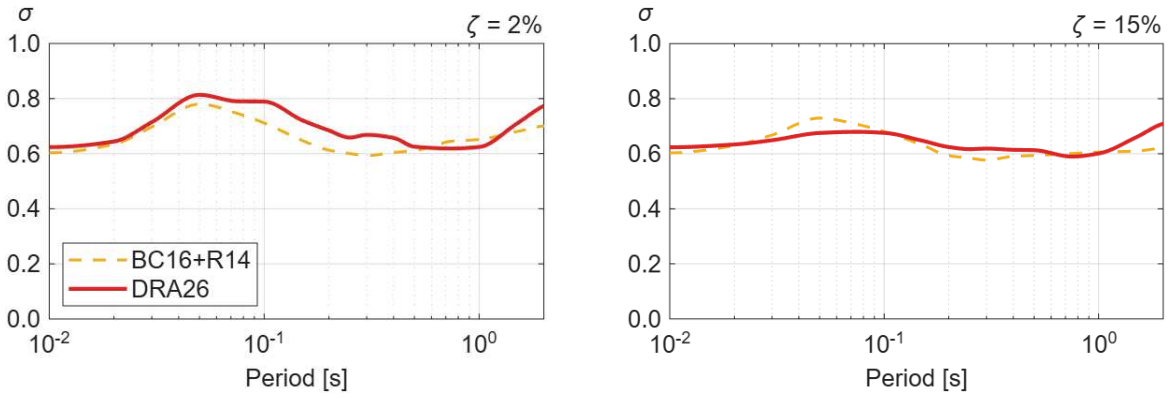
A comparison of the logarithmic standard deviations of Sa_v from both models is presented in Figure 8. For the implementation of the BC16+R14 compound model, the correlation coefficients between $ln\, Sa_V$ and $ln\, DSF_V$ are assumed to be those reported in Rezaeian et al. (2012) for $ln\, Sa_H$ and $ln\, DSF_H$ following recommendations by Rezaeian et al. (2014). Recall that these were derived from records with distances smaller than 50 km. This undoubtedly introduces some level of bias in the estimations of σ_{lnSav} and highlights the scarcity of access to the required correlation coefficients, a requirement that, while seemingly minor, is strictly mandatory for the process. The figure presents similar trends in the estimated variability between the two models. Both models suggests a slightly larger level of variability for lower damping ratios than for larger ones. This trend might be expected due to the jaggedness of elastic response spectra at lower damping ratios. This damping dependent-variability is an important advantage of the model.



331

332

333 ***Figure 7.*** *Comparison of median Sa_v ordinates between the proposed GMM and the indirect method for four*
334 *R_{jb}-M_w scenarios and for damping ratios of 1, 2, 10 and 20%.*



335

336 ***Figure 8.*** *Comparison of σ_{lnSav} between the proposed GMM and the indirect method for ζ = 2% and 15%.*

337 ## 6. Summary and Conclusions

338 This paper presented a damping-dependent ground-motion prediction model, GMM, for estimating vertical
339 pseudo-acceleration response spectra, Sa_v, for shallow crustal earthquakes recorded on firm soil sites. The
340 model was developed using a database of 2,408 vertical ground-motion records from earthquakes with
341 moment magnitudes (M_w) greater than 5.5 and Joyner–Boore distances shorter than 300 km. Response

spectra were computed at 17 vibration periods between 0.1 and 2.0 s for single-degree-of-freedom systems with damping ratios of 1, 2, 5, 10, 15, and 20%. The predictive capability of the model was evaluated using moment magnitude and Joyner–Boore distance as predictor variables through analyses of model residuals and logarithmic standard deviations. Based on the results, the model is suggested to be used for the estimation of Sa_v from active crustal earthquakes with M_w between 5 and 8, distances up to 200 km and for NEHRP site class D sites.

Predictions of the median S_{av} and its associated logarithmic standard deviation obtained with the proposed GMM were compared with those from an indirect approach combining the Bozorgnia and Campbell (2016b) GMM for the conventional 5%-damped vertical response spectrum with the vertical damping scaling model of Rezaeian et al. (2014) (hereafter referred to as the BC16+R14 approach). At a distance of 10 km, the proposed model predicts Sa_v ordinates that are, on average, 31.4% lower for a moderate earthquake (M_w = 6.5), but 19.9% higher for a large earthquake (M_w = 7.5) than those predicted with the BC16+R14 indirect approach. In both magnitude scenarios, the differences between the two models decrease as distance increases.

The results demonstrate that direct prediction of damping-dependent vertical response spectra constitutes a practical alternative to indirect damping-scaling procedures. With regards to the spectral variability in the median estimations, the proposed model offers a more consistent characterization, particularly for systems with effective damping ratios substantially different from the conventional 5% value. This is because the proposed direct model does not rely on correlation approximations but explicitly computes the variability in a single regression.

7. Acknowledgements

The authors are grateful to PEER and the corresponding networks and agencies for gathering, processing, and distributing these records. The third author acknowledges financial support by Universidad Panamericana to conduct his graduate studies under the supervision of the first author. The first and second authors would like to thank the Universidad Panamericana and the Universidad Michoacana de San Nicolás de Hidalgo, respectively.

8. Compliance with Ethical Standards

Funding details

The authors declare that no funds, grants, or other support were received during the preparation of this manuscript.

Conflict of interest

The authors have no relevant financial or non-financial interests to disclose.

Authorship contributions

Conceptualisation: HD; Investigation: DA, HD; Methodology: DH, JRG; Formal analysis: DA, HD; Writing—original draft: HD, JRG; Writing—review and editing: HD, JRG.

9. References

Abrahamson NA, Youngs RR (1992) A stable algorithm for regression analyses using the random effects model. *Bull Seismol Soc Am* **82**(1):505–510.

Abrahamson NA, and Silva WJ (1996). Empirical Ground Motion Models, Section 4: Spectral scaling for other damping values. Report to Brookhaven National Laboratory.

Abrahamson NA, Silva WJ (1997) Empirical response spectral attenuation relations for shallow crustal earthquakes. *Seismol Res Lett* **68**(1):94–127.

Akkar S, Sandikkaya MA, Ay BÖ (2014) Compatible ground-motion prediction equations for damping scaling factors and vertical-to-horizontal spectral amplitude ratios for the broader Europe region. *Bull Earthquake Eng* **12**:517–547.

Ambraseys NN, Douglas J (2003) Near field horizontal and vertical earthquake ground motions. *Soil Dyn Earthq Eng* **23**(1):1–18.

Ambraseys NN, Simpson KA (1996) Prediction of vertical response spectra in Europe. *Earthq Eng Struct Dyn* **25**(4):401–412.

Ancheta TD, Darragh RB, Stewart JP, Seyhan E, Silva WJ, Chiou BS-J, Wooddell KE, Graves RW, Kottke AR, Boore DM, Kishida T, Donahue JL (2014) NGA-West2 database. *Earthq Spectra* **30**(3), 989-1005.

Bommer JJ, Akkar S, Kale Ö (2011) A model for vertical-to-horizontal response spectral ratios for Europe and the Middle East. *Bull Seismol Soc Am* **101**(4):1783–1806.

Boore D, Atkinson G (2008) Ground-Motion Prediction Equations for the Average Horizontal Component of PGA, PGV, and 5%-Damped PSA at Spectral Periods between 0.01 s and 10.0 s. *Earthq Spectra* **24**(1); 99–138.

Bozorgnia Y, Campbell KW (2004) The vertical-to-horizontal response spectral ratio and tentative procedures for developing simplified V/H and vertical design spectra. *J Earthq Eng* **8**:175–207..

Bozorgnia Y, Campbell KW (2016a) Ground motion model for the vertical-to-horizontal (V/H) ratios of PGA, PGV, and response spectra. *Earthq Spectra* **32**(2):951–978.

Bozorgnia Y, Campbell KW (2016b) Vertical ground motion model for PGA, PGV, and linear response spectra using the NGAWest2 database. *Earthq Spectra* **32**(2):979–1004.

Bozorgnia Y, Niazi M, & Campbell KW (1995) Characteristics of free-field vertical ground motion during the Northridge earthquake. *Earthq Spectra* **11**(4): 515–525.

Brillinger DR, Preisler HK (1984) An exploratory analysis of the Joyner-Boore attenuation data. *Bull Seismol Soc Am* **74**(4):1441–50.

Brillinger DR, Preisler HK (1985) Further analysis of the Joyner-Boore attenuation data. *Bull Seismol Soc Am* **75**(2):611–4.

Campbell KW (1997) Empirical near-source attenuation relationships for horizontal and vertical components of peak ground acceleration, peak ground velocity, and pseudo-absolute acceleration response spectra. *Seismol Res Lett* **68**:154–179.

Campbell KW (2001) Erratum: empirical near-source attenuation relationships for horizontal and vertical components of peak ground acceleration, peak ground velocity, and pseudo-absolute acceleration response spectra. *Seismol Res Lett* **72**:474.

Campbell KW, Bozorgnia Y (2003) Updated near-source ground-motion (attenuation) relations for the horizontal and vertical components of peak ground acceleration and acceleration response spectra. *Bull Seismol Soc Am* **93**(1):314–331.

Chiou BS-J, Youngs RR (2008) An NGA Model for the Average Horizontal Component of Peak Ground Motion and Response Spectra. *Earthq Spectra* **24**(1): 173–215.

Campbell KW, Bozorgnia Y (2016) NGA ground motion model for the geometric mean horizontal component of PGA, PGV, PGD and 5% damped linear elastic response spectra for periods ranging from 0.01 to 10 s. *Earthq Spectra* **24**(1): 139-171.

Chiou BS-J, Youngs RR (2013) NGA-West2 ground motion prediction equations for vertical ground motions. PEER Report 2013/24, Pacific Earthquake Engineering Research Center, Berkeley, CA, pp 127–161.

Çagnan Z, Akkar S, Kale Ö, Sandıkkaya MA (2017) A model for predicting vertical component peak ground acceleration (PGA), peak ground velocity (PGV), and 5% damped pseudo spectral acceleration (PSA) for Europe and the Middle East. *Bull Earthquake Eng* 15(7):2617–2643.

Elnashai AS, Papazoglou AJ (1997) Procedure and spectra for analysis of RC structures subjected to strong vertical earthquake. *J Earthq Eng* **1**(1):121–155.

Gülerce Z, Abrahamson NA (2011) Site-specific design spectra for vertical ground motion. *Earthq Spectra* **27**:1023–1047.

Gülerce Z, Kamai R, Abrahamson NA, Silva WJ (2017) Ground motion prediction equations for the vertical ground motion component based on the NGA-W2 database. Earthquake Spectra 33 (2): 499-528.

Dominguez H, Heresi P, Montalva G, and Leyton F (2025). Vertical ground motion model for PGA and spectral accelerations for the Chilean subduction zone. Bull of Earthq Eng. Under Review.

Hu L, Li Y, Pan W, Yang H, Ji S (2025) A damping scaling factor model for vertical elastic response spectra from subduction earthquakes in offshore and onshore regions of Japan. *Soil Dyn Earthq Eng* **193**:109322.

Kunnath SK, Erduran E, Chai YH, & Yashinsky M. (2008) Effect of near-fault vertical ground motions on seismic response of highway overcrossings. *Journal of Bridge Eng*, **13**(3): 282-290.

Laouami N (2019) Vertical ground motion prediction equations and vertical-to-horizontal (V/H) ratios of PGA and PSA for Algeria and surrounding region. *Bull Earthquake Eng* **17**(7):3637–3660.

Malhotra PK (2006) Smooth spectra of horizontal and vertical ground motions. *Bull Seismol Soc Am* **96**:505–518.

McGuire RK, Silva WJ, Costantino CJ (2001) Technical basis for revision of regulatory guidance on design ground motions: hazard- and risk-consistent ground motion spectra guidelines, Section 4.9: Estimation of spectra for other dampings. Report NUREG/CR-6728, Prepared for Division of Engineering Technology, Office of Nuclear Regulatory Research, U.S. Nuclear Regulatory Commission, Washington, D.C.

Niazi M, Bozorgnia Y (1991) Behavior of near-source peak horizontal and vertical ground motions over SMART-1 array, Taiwan. *Bull Seismol Soc Am* **81**(3):715–732.

Niazi M, Bozorgnia Y (1992) Behavior of near-source vertical and horizontal response spectra at SMART-1 array, Taiwan. *Earthq Eng Struct Dyn* **21**(1):37–50.

Papazoglou AJ, Elnashai AS (1996) Analytical and field evidence of the damaging effects of vertical earthquake ground motion. *Earthq Eng Struct Dyn* **25**:1109–1137.

Phung V-B, Abrahamson NA, Huang B-S, Loh C-H (2022) Vertical ground-motion prediction equation and the vertical-to-horizontal spectral ratio for crustal earthquakes in Taiwan. *Earthq Spectra* **38**(2):1–34.

Ramadan F, Pittore M, Weatherill G, Cotton F (2021) An empirical model for the vertical-to-horizontal spectral acceleration ratio for earthquakes in the European and Middle Eastern regions. *Earthq Eng Struct Dyn* **50**(13):3462–3483.

Rezaeian S, Bozorgnia Y, Idriss IM, Campbell K, Abrahamson N, Silva W (2012) Spectral damping scaling factors for shallow crustal earthquakes in active tectonic regions. PEER Report 2012/102, Pacific Earthquake Engineering Research Center, Berkeley, CA.

Rezaeian S, Bozorgnia Y, Idriss IM, Abrahamson NA, Campbell KW, Silva WJ (2014) Damping scaling factors for vertical elastic response spectra for shallow crustal earthquakes in active tectonic regions. *Earthq Spectra* **30**:1335–1358.

Rezaeian S, Al Atik L, Kuehn NM, Abrahamson N, Bozorgnia Y, Mazzoni S, ... & Campbell K. (2021). Spectral damping scaling factors for horizontal components of ground motions from subduction earthquakes using NGA-Subduction data. *Earthq Spectra* **37**(4): 2453-2492.

Stewart JP, Boore DM, Seyhan E, Atkinson GM (2016) NGA-West2 equations for predicting vertical-component PGA, PGV, and 5%-Damped PSA from Shallow Crustal Earthquakes. *Earthq Spectra* **32**(2):1005–1031.

Wibowo H, Sritharan S (2022) Effects of vertical ground acceleration on the seismic moment demand of bridge superstructure connections. *Engineering Structures* **253**: 113820.